Structural Role of Glycine in Amyloid Fibrils Formed from Transmembrane α-Helices†

Wei Liu,‡ Evan Crocker,§ Wenyi Zhang,‡ James I. Elliott,|| Burkhard Luy,⊥ Huilin Li,▽ Saburo Aimoto,○ and Steven O. Smith*,‡

Departments of Biochemistry and Cell Biology and of Physics and Astronomy, Center for Structural Biology, Stony Brook University, Stony Brook, New York 11794-5215, Department of Molecular Biophysics and Biochemistry, Yale University, New Haven, Connecticut 06520-8024, Technische Universitaet München, D-85747 Garching, Germany, Department of Biology, Brookhaven National Laboratory, Upton, New York 11973, and Institute for Protein Research, Osaka University, 3-2 Yamadaoka, Suita, Osaka 565-0871, Japan

Received October 8, 2004; Revised Manuscript Received December 9, 2004

ABSTRACT: Amyloid fibrils associated with diseases such as Alzheimer's are often derived from the transmembrane helices of membrane proteins. It is known that the fibrils have a cross-β-sheet structure where main chain hydrogen bonding occurs between β-strands in the direction of the fibril axis. However, the structural basis for how the membrane-spanning helix is converted into a β-sheet or how protofibrils associate into fibrils is not known. Here, we use a model peptide corresponding to a portion of the single transmembrane helix of glycophorin A to investigate the structural role of glycine in amyloid-like fibrils formed from transmembrane helices. Glycophorin A contains a GxxxG motif that is found in many transmembrane sequences including that of the amyloid precursor protein and prion protein. We propose that glycine, which mediates helix interactions in membrane proteins, also provides key packing motifs when it occurs in β-sheets. We show that glycines in the glycophorin A transmembrane helix promote extended β-strand formation when the helix partitions into aqueous environments and stabilize the packing of β-sheets in the formation of amyloid-like fibrils. We demonstrate that fibrillization can be disrupted with a new class of inhibitors that target the molecular grooves created by glycine.

Aggregation and deposition of misfolded protein are characteristic of neurodegenerative disorders as diverse as Alzheimer's disease and transmissible spongiform encephalopathies. In many cases, the amyloidogenic peptide sequences originate from the transmembrane helices of membrane proteins. For instance, the insoluble plaques characteristic of Alzheimer's disease are formed from amyloid-β (Aβ) peptides (Figure 1A) with lengths varying from 38 to 43 amino acids (*1*, *2*). These peptides are generated by the action of two proteases on the Amyloid Precursor Protein (APP[1]). APP is a transmembrane protein of unknown function with a single membrane-spanning helix. β-Secretase cleaves within the extracellular sequence of the protein, while γ-secretase cleaves within the membrane-spanning sequence (*3*, *4*). As a result, the Aβ_{1-42} peptide incorporates ∼65%

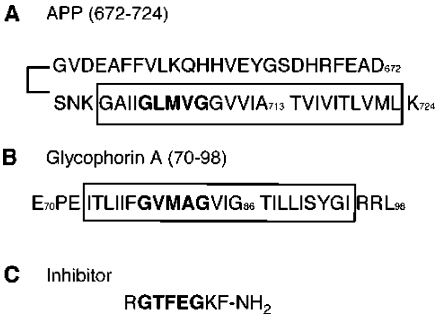

FIGURE 1: Glycine-rich peptide sequences involved in the formation and inhibition of amyloid fibrils. (A) Sequence of the APP from Asp672 to Lys724. The Aβ_{1-42} peptide that forms amyloid fibrils in Alzheimer's disease corresponds to Asp672 to Ala713 of APP. The C-terminus of the Aβ_{1-42} peptide corresponds to a large part of the APP transmembrane domain (boxed). γ-Secretase releases the 42-residue peptide by cleaving in the middle of the transmembrane domain, 10 amino acids from the cytoplasmic end of the transmembrane sequence. (B) Sequence of glycophorin A from Glu70 to Leu98. The transmembrane domain (boxed) of glycophorin A (Glu70−Leu98) spans membrane bilayers in α-helical secondary structure. Truncating the sequence at Gly86 mimics the hydrophobic C-terminus of Aβ_{1-42} and results in a peptide that is not long enough to span membrane bilayers. Gly86 is nine amino acids before an arginine which defines the cytoplasmic end of the transmembrane sequence. (C) Sequence of a designed eight amino acid peptide inhibitor. In bold is a GxxxG motif contained in all three peptides.

† This work was supported by a research grant to S.O.S. from the NIH (GM-46732) and NIH-NSF instrumentation grants (S10 RR13889 and DBI-9977553). We gratefully acknowledge the W.M. Keck Foundation for support of the NMR facilities in the Center of Structural Biology at Stony Brook.

* To whom correspondence should be addressed. Phone: (631) 632-1210. Fax: (631) 632-8575. E-mail: steven.o.smith@sunysb.edu.

‡ Department of Biochemistry and Cell Biology, Stony Brook University.

§ Department of Physics and Astronomy, Stony Brook University.

|| Yale University.

⊥ Technische Universitaet München.

▽ Brookhaven National Laboratory.

○ Osaka University.

[1] Abbreviations: APP, amyloid precursor protein; DARR, dipolar assisted rotational resonance; DMPC, 1,2-dimyristoyl-*sn*-glycero-3-phosphocholine; EM, electron microscopy; FTIR, Fourier transform infrared; MAS, magic angle spinning; NMR, nuclear magnetic resonance; ThT, thioflavin T; TM, transmembrane.

10.1021/bi047827g CCC: $30.25
Published on Web 02/10/2005

(residues 700−713) of the transmembrane domain of APP. Importantly, it is this hydrophobic C-terminal stretch of 14 amino acids which is thought to be the seed or nucleation site for fibril formation (*5*).

Several structural transformations occur to convert a membrane-spanning α-helix to a soluble peptide with random coil or extended β-strand structure, and subsequently to a fibril with cross-β-sheet structure. Glycine, which has a striking prevalence in the transmembrane segments of APP, may potentiate these structural changes. First, glycine is known to function as a flexible hinge to disrupt α-helical secondary structure in aqueous environments, and consequently is often the key design element in proteins that have been engineered to convert from an α-helix to a β-sheet (*6*). Second, glycine has a higher preference for β-sandwich folds than for β-sheet alone (see the Discussion) and stabilizes sheet-to-sheet packing.

In the past few years, we have shown that glycine plays a major role in mediating helix−helix interactions in membrane proteins (*7*, *8*). Glycine has a high occurrence in hydrophobic membrane-spanning helices, where it facilitates helix association by acting as a molecular notch (*7*, *8*). Glycine occurs in the context of many different sequence motifs to mediate dimerization (*8*). These sequence motifs contain at least one glycine and are strongly hydrophobic. One such sequence motif, the GxxxG motif, was identified by Engelman and co-workers (*9*) and shown to mediate dimerization in TOXCAT screens of transmembrane libraries (*10*). The GxxxG motif places the two glycines on the same side of a helix or on the same face of a β-sheet. The absence of a bulky side chain results in a molecular notch in both secondary structures.

We use the glycine-rich transmembrane helix of glycophorin A to test the proposal that helix-forming, hydrophobic transmembrane peptides rich in glycine can spontaneously adopt β-structure and form fibrils when truncated. Glycophorin A is a major protein of erythrocyte membranes. The single membrane-spanning helix of glycophorin A contains several glycines that mediate dimerization and has been extensively studied by mutational (*11*) and structural (*12*, *13*) analysis. There has been no suggestion previously that peptides incorporating all or part of the glycophorin A transmembrane sequence would be able to form amyloid-like fibrils.

We describe three different approaches for addressing the structural role of glycine in the formation of amyloid-like fibrils. First, we show that the helical transmembrane domain of glycophorin A adopts β-structure when it is truncated by 40% and is no longer able to span membrane bilayers. The 17-residue hydrophobic sequence, corresponding to amino acids 70−86 of glycophorin A, associates into β-sheets and forms amyloid-like fibrils. Second, we use solid-state NMR spectroscopy to show that the individual β-strands have a parallel, in-register orientation within a β-sheet and that sheet-to-sheet packing involves large hydrophobic amino acids (e.g., methionine) packing into the surface notches or grooves created by glycine. Third, on the basis of these findings we have designed peptides that are able to inhibit fibril formation of the truncated glycophorin A peptide. These data indicate that glycine in a sequence containing mostly hydrophobic and β-branched amino acids may be key to the formation of insoluble β-sheet structure from transmembrane sequences that do not correctly insert into membranes or have been enzymatically cleaved and no longer span membrane bilayers.

MATERIALS AND METHODS

Peptide Synthesis, Purification, and Fibrillization. Peptides were synthesized on an ABI 430A solid-phase peptide synthesizer (Applied Biosystems, Foster City, CA) using tBOC chemistry. Hydrofluoric acid was used for cleavage and deprotection. Peptide purification was achieved by reverse-phase HPLC using linear water−acetonitrile gradients containing 0.1% trifluoroacetic acid. The purity was confirmed by mass spectrometry.

For fibrillization, peptides were first dissolved in hexafluoro-2-propanol and incubated at 25 °C for 30 min. The organic solvent was then evaporated by a flow of argon gas, and the samples were lyophilized. Samples for NMR and fluorescence experiments were prepared by incubation of aqueous solutions at peptide concentrations of approximately 0.2 mM (NMR) or 80 μM (fluorescence) in 5.0 mM phosphate buffer at pH 7.4 with the pH adjusted as necessary by dropwise addition of dilute NaOH or HCl. NaN_3 (0.01%) was added to inhibit bacterial and fungal growth. The solutions were incubated for 6−14 days at a temperature of 25 °C with gentle shaking (200 rpm). The solutions form a gel as the amyloid-like fibrils form. Fibril formation was verified by electron microscopy (EM) of negatively stained samples and fluorescence spectroscopy. Fibrils were concentrated by centrifugation to keep the peptides hydrated for solid-state NMR measurements.

FTIR Spectroscopy. FTIR spectra were obtained on a Bruker IS 66V/S spectrometer. Peptides were first cosolubilized with octyl β-glucoside and DMPC, and then the detergent was removed by dialysis. The resulting multilamellar vesicle dispersions at a concentration of 10 mg of lipid/mL were layered on a germanium internal reflection element, and bulk water was removed using a slow flow of N_2 gas to form a multilamellar lipid−peptide film.

Electron Microscopy. For fibril observation, a 5 μL sample of the peptide was placed on a carbon film coated 300 mesh copper grid. The sample was allowed to stand for 15−30 s, and any excess solution was wicked away. The samples were negatively stained with 2% (w/v) uranyl acetate. The excess was wicked away and the sample allowed to dry. The samples were then visualized under a JEOL 1200EX transmission electron microscope operating at 120 kV at a magnification of 50000×. For electron diffraction of frozen hydrated fibers, the sample was concentrated by low-speed centrifugation for 10 min, and vitrified by plunge-freezing the grids into liquid ethane. Diffraction patterns were recorded on a Tietz 2K-by-2K CCD camera in a JEOL 2010F FasTEM operated at 200 kV. Sample grids were kept at −170 °C and imaged under low-dose conditions.

Fluorescence Spectroscopy. Measurements of thioflavin T (ThT) fluorescence (*14*) were performed daily for 6 days using a Jacob FP-6200 spectrometer with excitation and emission wavelengths of 450 nm (5 nm slit width) and 482 nm (5 nm slit width), respectively. The inhibitor peptide was solubilized in 5 mM phosphate buffer (pH 7.4) to a final concentration of 4 mM. GpA_{70-86} peptides were mixed with the inhibitor to obtain peptide-to-inhibitor molar ratios of

1:1 to 1:20. The solution was diluted with phosphate buffer to a final volume of 6 mL and incubated at 25 °C with gentle agitation (200 rpm). ThT fluorescence measurements were made by mixing 0.35 mL of the GpA−inhibitor solution with 0.35 mL of 0.2 mM ThT. Each experiment was carried out in triplicate.

Solid-State NMR Spectroscopy. Solid-state 2D NMR measurements were made on either a 360 or a 600 MHz Bruker AVANCE spectrometer using 4 mm MAS probes. The MAS spinning rate was set to eliminate overlap of ^{13}C cross-peaks with MAS sidebands in the 2D recoupling experiments. Ramped amplitude cross-polarization (*15*) contact times were 2 ms in all experiments, and two-pulse phase-modulated (*16*) decoupling was used during the evolution and acquisition periods. The decoupling field strength was typically 90 kHz. ^{13}C chemical shifts were referenced to external tetramethylsilane. Solid-state NMR samples contained 3−10 mg of peptide.

For DARR experiments (*17*), mixing times of 600 ms to 1 s were used to maximize homonuclear recoupling between ^{13}C labels (*18*). The ^{1}H radio frequency field strength during mixing was matched to the spinning speed to satisfy the $n = 1$ condition for each sample. Each 2D data set represents 1K to 5K scans in each of 64 rows in the f1 dimension. An exponential line broadening of 10 Hz was used in the f2 dimension, and a cosine multiplication was used in the f1 dimension along with a 32-coefficient forward linear prediction.

Sequence Analysis. We tabulated the occurrence of amino acids in β-sheet secondary structure in the 20 representative (unique) proteins comprising the β-sandwich family as defined by the CATH database (Architecture 2.60) (*19*). The amino acid preferences in the β-sandwich fold were calculated as the percentage of each amino acid having β-structure in the β-sandwich fold. The amino acid preferences for β-sheet secondary structure were obtained from the literature (*20*).

RESULTS

Truncated Glycophorin A Forms Amyloid-like Fibrils. The glycophorin A transmembrane sequence (Figure 1B) contains four glycines and is known to form a well-defined α-helix in membrane bilayers (*21*). We have shown previously that Gly79 and Gly83 mediate dimerization of the full-length glycophorin A transmembrane helix by acting as molecular notches (*13*). Figure 2A presents Fourier transform infrared (FTIR) spectra of the full-length and truncated glycophorin A peptides immediately following reconstitution with lipid bilayers (i.e., before fibril formation). The full-length transmembrane sequence, GpA_{70-98}, folds into an α-helix as characterized by an amide I vibration at 1657 cm^{-1}. On the basis of the dichroic ratio of the amide I band, the GpA_{70-98} helix inserts into DMPC bilayers in a transmembrane orientation (*21*) (data not shown). In striking contrast, the truncated GpA_{70-86} peptide, which is no longer able to span the bilayer, adopts almost exclusively β-structure characterized by an amide I vibration at 1625 cm^{-1}.

Amyloid fibrils formed from the Aβ peptides in Alzheimer's disease typically take 2−3 days to appear in a solution of peptide monomers. EM images obtained of the glycophorin peptides after 3 days reveal that the truncated GpA_{70-86} peptide forms fibrils similar in size and appearance to those produced by $A\beta_{1-42}$ (Figure 2B). As with the Aβ peptides, the GpA_{70-86} fibrils are able to form in either the presence or the absence of membranes. In contrast, the full-length transmembrane peptide does not form fibrils in the presence of membranes. In the absence of membranes, the full-length GpA_{70-98} peptide forms insoluble aggregates.

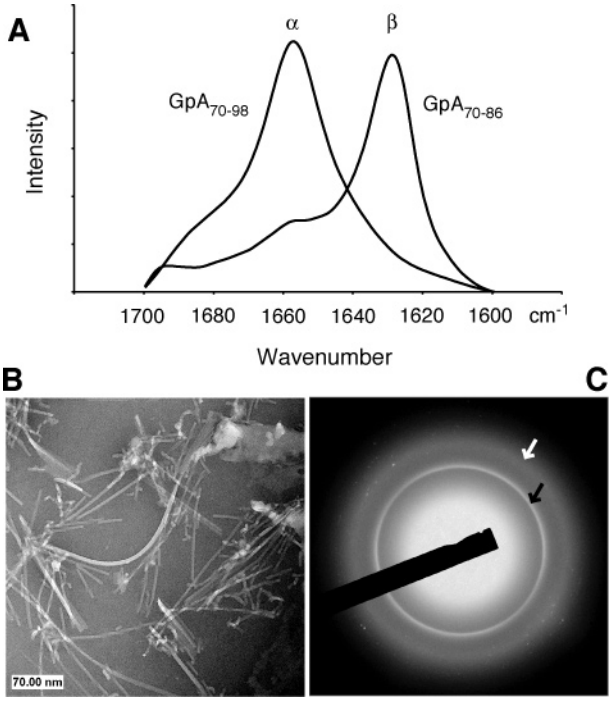

FIGURE 2: Fibril formation of GpA_{70-86}. (A) FTIR spectra of the amide I region of the full-length GpA_{70-98} and truncated GpA_{70-86} peptides reconstituted with DMPC lipids. The full-length GpA_{70-98} peptide adopts helical secondary structure and inserts into DMPC bilayers in a transmembrane orientation (*21*), while the GpA_{70-86} is unable to span membrane bilayers and adopts primarily β-structure. (B) Electron micrograph of the fibrils formed by the truncated GpA_{70-86} peptide. Amyloid-like fibrils of the GpA_{70-86} peptide are observed if the peptide is incubated with or without membrane lipids. (C) Electron diffraction pattern of GpA_{70-86} fibrils showing the 4.7 Å ring (black arrow) characteristic of the spacing between β-strands in β-sheet secondary structure. The outer ring at 3.6 Å (white arrow) is due to amorphous ice. The 4.7 Å feature was not observed in control samples without fibrils or in areas away from the fibril bundles.

It is known that amyloid fibrils formed from $A\beta_{1-42}$ have a cross-β-sheet structure where the β-strands hydrogen bond along the direction of the fibril or protofibril axis (*22*). To show that the fibrils observed in the EM images of GpA_{70-86} also contain β-structure, electron diffraction patterns were collected from frozen fibrils. The GpA_{70-86} fibrils reveal a strong diffraction ring at 4.7 Å (Figure 2C) consistent with the strand-to-strand repeat in β-sheets. The ring was not observed in control samples without peptide or in the nearby regions of the sample grid that did not contain fibrils.

To test whether glycines are involved in the transition from α-helix to β-strand secondary structure when the GpA peptides are truncated, peptides were synthesized with individual glycines replaced with alanine. This was the most conservative mutation possible. The truncated GpA_{70-86} peptide with Gly79Ala and Gly83Ala substitutions was not soluble in the presence or absence of membranes, and consequently did not adopt β-strand structure or form fibrils (data not shown).

Glycine Facilitates Dovetail Packing in Amyloid Fibrils. The formation of fibrils from peptide monomers involves at least two steps that may or may not be independent: the backbone carbonyl and amide groups of monomeric β-strands hydrogen-bond in the direction parallel to the fibril axis to form β-sheets, and the β-sheets associate in the direction perpendicular to the fibril axis to form protofibrils and fibrils. To establish if glycine is involved in these steps, high-resolution structures of the fibrils are needed. Unfortunately, detailed fibril structures cannot be determined by X-ray crystallography or by high-resolution solution NMR due to the insoluble nature of the samples.

Several groups have shown that high-resolution structural constraints can be obtained using solid-state NMR spectroscopy (*23*−*25*). The focus in these studies has been on defining the secondary structure of the peptides and how the β-strands are oriented relative to one another *within* a β-sheet. In Aβ_{1-40}, the individual β-strands have a parallel N-to-C orientation and the side chains are in-register within a sheet (*26*). The amino acid sequence of the GpA$_{70-86}$ peptide is similar to the sequence of the C-terminal portion of Aβ_{1-40} and Aβ_{1-42} (Figure 1A,B), and we propose that a similar packing arrangement occurs in these peptides.

To test whether the individual β-strands in GpA$_{70-86}$ fibrils have a parallel orientation within a β-sheet, two-dimensional (2D) solid-state NMR measurements were performed on GpA$_{70-86}$ fibrils containing specifically ^{13}C-labeled glycine. For these experiments, fibrils were formed using equimolar amounts of two peptides with ^{13}C labels at different positions in the GpA$_{70-86}$ sequence. The first peptide was labeled at the α-carbons and carbonyl carbons of Gly79 and Gly83, respectively, while the second peptide was labeled at the α-carbons and carbonyl carbons of Gly83 and Gly79, respectively. These α-carbons and carbonyl carbons are >14 Å apart within each individual (extended) peptide, but are predicted to be ∼3.5 Å from one another if the peptides have a parallel orientation within a β-sheet (Figure 3B).

Figure 3A presents the 2D NMR spectrum of the GpA$_{70-86}$ fibrils containing α-carbon and carbonyl-labeled glycine. It was obtained using dipolar-assisted rotational resonance (DARR) (*27*), which gives rise to off-diagonal cross-peaks if the ^{13}C labels are separated by less than ∼5.5 Å. Both the α-carbon and carbonyl carbon resonances for Gly79 and Gly83 are resolved along the diagonal of the 2D NMR spectrum. We have previously shown that the intensities of cross-peaks between dipole-coupled spins in the DARR experiment are roughly proportional to their internuclear distance (*18*). On the basis of these studies, the intensities of the cross-peaks (boxed) between the α-carbon and carbonyl carbon resonances are consistent with their predicted 3.5 Å interstrand distance, indicating that the peptides in the fibrils have a parallel, in-register orientation (Figure 3B). Cross-peaks would not have been observed if the peptides were not parallel or in-register.

The observation of a parallel, in-register structure for the β-strands means that the alternating large and small side chains produce a series of ridges and grooves which run the length of the fibril (Figure 4). The long hydrophobic grooves created by glycines raise the possibility that sheet-to-sheet packing in protofibrils and fibrils may be stabilized by a ridges-into-grooves packing arrangement that is remarkably similar to the type of packing interaction mediated by

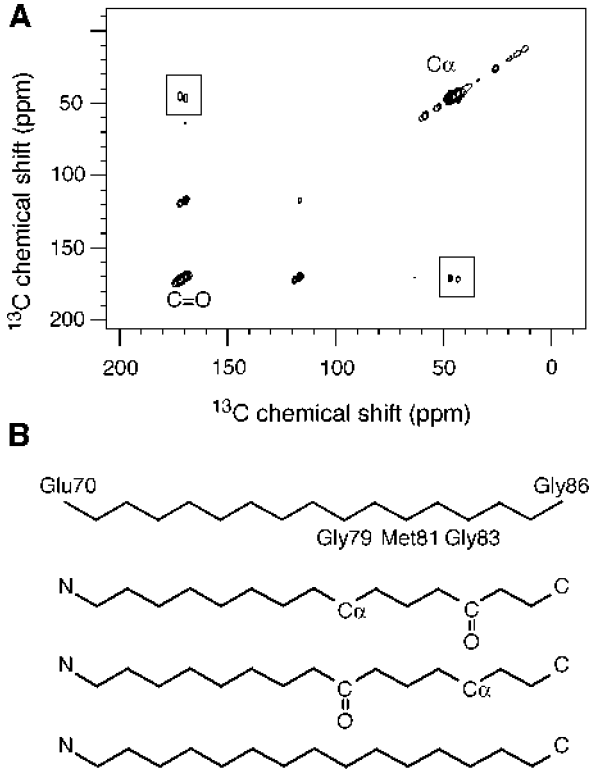

FIGURE 3: Solid-state magic angle spinning NMR of GpA$_{70-86}$ fibrils. (A) 2D DARR NMR spectrum of GpA$_{70-86}$ formed from an equimolar mixture of [1-^{13}C]Gly79,[2-^{13}C]Gly83-labeled peptide and [2-^{13}C]Gly79,[1-^{13}C]Gly83-labeled peptide. Cross-peaks between the 1-^{13}C and 2-^{13}C resonances are consistent with a parallel, in-register orientation of the peptides within a β-sheet. (B) Proposed cross β-structure of GpA$_{70-86}$ fibrils with the individual β-strands having a parallel N-to-C orientation. The amino acids are in-register with one another between strands. The positions of the ^{13}C-labeled carbons on Gly79 and Gly83 are shown. The interstrand Cα-to-C═O distances are ∼3.5 Å.

glycines in transmembrane helix dimers (*28*). In fact, we propose that the large side chains on one β-sheet *dovetail* into the grooves formed by glycine on an opposing β-sheet. To test this idea, we incorporated a single ^{13}C isotope label at the backbone carbonyl carbon of Gly79 in the GpA$_{70-86}$ peptide and measured its intermolecular distance to the ^{13}C-labeled side chain methyl group of Met81 on adjacent β-sheets by solid-state NMR. Modeling of the β-sandwich formed from the GpA$_{70-86}$ peptide predicts an *inter*-β-sheet distance of 3−5 Å between the carbonyl ^{13}C of Gly79 and the ^{13}CH$_3$ of Met81. The *intra*sheet distance between these amino acids is ∼8−10 Å, outside the detection range of the NMR experiment used.

Figure 5A presents a slice of the 2D DARR NMR spectrum of fibrils formed by the GpA$_{70-86}$ peptide using an equimolar mixture of [^{13}CH$_3$]Met81-labeled peptide and [1-^{13}C]Gly79-labeled peptide. A well-defined cross-peak is observed between Met81 and Gly79 which is absent in fibrils formed using only peptides containing ^{13}C-labeled Met81 (Figure 5B). The observed intensity of this cross-peak indicates that the side chain of Met81 is within 5 Å of Gly79 on an opposing β-sheet. This supports the proposal that Met81 packs in the groove created by Gly79 in a dovetail fashion (Figure 4).

A Designed Peptide Based on Dovetail Packing Inhibits Fibril Formation. The results above provide the structural

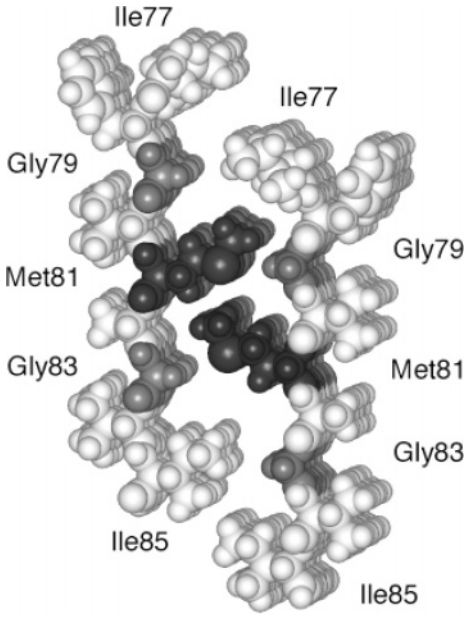

FIGURE 4: Dovetail packing within GpA_{70-86} fibrils. The parallel, in-register stacking of β-strands within a β-sheet creates long channels at the position of glycine (dark gray). The channels run in the direction of the fibril axis (out of the page). The long hydrophobic side chain of Met81 (black) packs in a dovetail or Ziploc fashion into the grooves created by Gly79 and Gly83. For clarity, the two β-sheets are separated from one another and only the amino acids from Ile77 to Ile85 are shown. The remainder of the sequence is presumed to contribute to the β-sheet structure that forms the fibrils observed by EM.

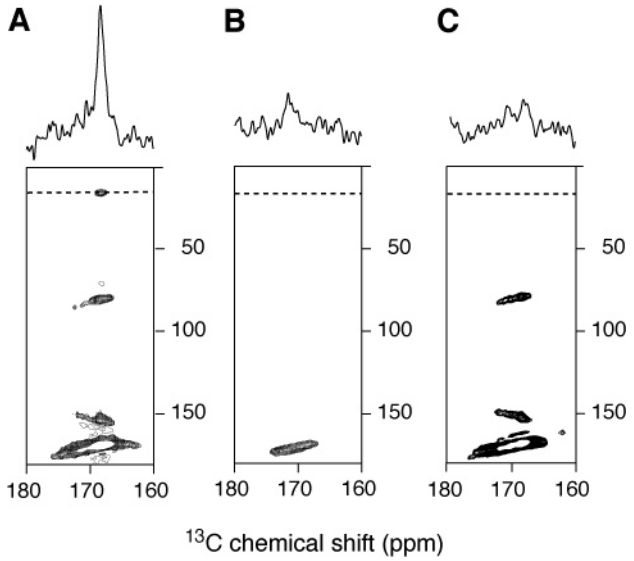

FIGURE 5: Solid-state magic angle spinning NMR of GpA_{70-86} fibrils. (A) 2D DARR NMR spectrum of GpA_{70-86} fibrils formed from an equimolar mixture of [$^{13}CH_3$]Met81-labeled peptide and [1-^{13}C]Gly79-labeled peptide. The cross-peak observed between Met81 and Gly79 is consistent with dovetail sheet-to-sheet packing. (B) 2D NMR spectrum of fibrils containing only the [$^{13}CH_3$]Met81-labeled peptide. The carbonyl signal is less intense here because only the natural abundance ^{13}C signal is observed. (C) 2D NMR spectrum obtained of the equimolar mixture of peptides in (A) incubated with an equimolar amount of the eight amino acid inhibitor RGTFEGKF-NH_2. One-dimensional slices at the position of the dashed line are shown at the top of the figures.

basis for the rational design of a new class of inhibitors to block the formation of amyloid fibrils. Figure 1C shows the sequence of a designed eight amino acid inhibitor. In an extended β-strand conformation, one face of the inhibitor (G-F-G-F) is predicted to bind to the G-M-G face of GpA_{70-86}, with the bulky Phe side chains of the inhibitor packing against the glycine backbone of the peptide. The other face of the inhibitor (R-T-E-K) is charged and highly polar to increase the solubility of the peptide. To test the ability of the inhibitor to disrupt fibril formation by specifically binding to GpA_{70-86}, we incubated the inhibitor at an equimolar ratio with the GpA_{70-86} peptide. The peptide−inhibitor solutions did not form gels characteristic of fibril formation, and EM images obtained over the course of two weeks revealed no detectable fibrils. In contrast, parallel incubations of the GpA_{70-86} peptide without inhibitor produced abundant fibrils.

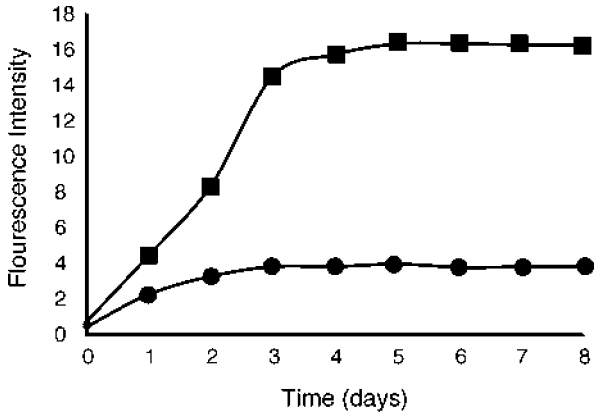

FIGURE 6: Inhibition of fibril formation by a designed peptide. The fluorescence intensity of ThT measured at 482 nm shows that GpA_{70-86} fibrils (squares) form in approximately 3 days. Addition of the designed inhibitor (RGTFEGKF-NH_2) at a GpA-to-inhibitor ratio of 1:20 reduces fibril formation by 80% (circles).

We also lyophilized the peptide−inhibitor solutions after incubation for two weeks and collected 2D DARR NMR spectra. For these measurements, we used an equimolar mixture of GpA_{70-86} peptides ^{13}C-labeled at Gly79 and Met81 (as in Figure 5A), but incubated with inhibitor at a 1:1 molar ratio of inhibitor to peptide. The NMR cross-peak observed in Figure 5A is not present after incubation with the inhibitor (Figure 5C), indicating that the inhibitor disrupts the Gly79−Met81 contact. These data provide indirect support of our proposal that the inhibitor binds in the surface grooves formed by glycine.

A more quantitative test of fibril formation and inhibition was carried out using the thioflavin T (ThT) fluorescence assay (*14*). Binding of ThT to amyloid fibrils results in increased fluorescence at 482 nm. For these measurements, we incubated the GpA_{70-86} peptide with the inhibitor at molar ratios ranging from 1:1 to 1:20. Figure 6 shows the formation of GpA_{70-86} fibrils (squares) as a function of time as monitored by increased ThT fluorescence. Addition of the eight-residue inhibitor reduces fibril formation by ~80% at a molar ratio of 1:20. Parallel experiments on the inhibition of $A\beta_{1-42}$ peptides by this inhibitor showed that a 1:20 molar ratio resulted in ~70% reduction in fibrillization (unpublished results). Inhibitors with glycine substituted with leucine did not block fibril formation.

DISCUSSION

Role of Glycine in Fibril Formation. The results above highlight three distinct features of glycine structure which

may contribute to the formation of insoluble fibrils by peptides derived from transmembrane sequences rich in glycine.

First, the lack of a side chain increases the flexibility of the polypeptide at the position of glycine. This is the textbook role of glycine in soluble protein sequences. We propose that glycine has the same role for amyloidogenic sequences and facilitates the α-helix-to-β-sheet transition of hydrophobic peptides that contain glycine and have partitioned out of the hydrophobic interior of membrane bilayers. Substitution of Gly79 and Gly83 with alanine is well tolerated in the full-length glycophorin A transmembrane domain, although it disrupts dimerization (*11*). However, in the truncated GpA_{70-86} peptide these substitutions lead to an insoluble peptide that does not adopt β-strand structure or form fibrils.

Second, we postulate that glycine can function as a molecular notch to stabilize sheet-to-sheet packing in amyloid fibrils. Sheet-to-sheet packing is a hallmark of the β-sandwich folding motif seen in many soluble proteins where at least two β-sheets stack on top of one another. To test whether there is a preference for glycine in β-sandwich folds over simple β-sheet secondary structure, we compared the distributions of amino acids between these structures using the CATH database (Architecture 2.60) (*19*), which catalogs known β-sandwich proteins. The amino acid preferences for β-sheet secondary structure were obtained from the literature (*20*). The amino acid preferences in 20 unique β-sandwich proteins identified in the CATH database (http://www.biochem.ucl.ac.uk/bsm/cath/) were calculated by taking the percentage of each amino acid found in the β-sandwich structure and dividing by 5%, the value if each of the 20 amino acids is equally represented. The propensity for glycine is significantly higher in β-sandwich structures (0.99) than in standard β-strand secondary structures (0.58). Generally, small and charged residues are found to have higher preferences for β-sandwich secondary structure, while large residues have a lower preference (see Table 1 in the Supporting Information). This distribution (and inspection of known β-sandwich structures) supports the idea that glycine (and small residues) can serve as molecular notches to stabilize β-sandwich secondary structure in much the same way as they stabilize the association of transmembrane helix dimers.

Third, β-sheets in high-resolution structures are generally observed to have an inherent twist. This is attributed to the chiral structure of all amino acids except glycine. β-sheets containing glycine are flattened due to the lack of side chain chirality (*29*), a feature which may aid the association of more than two β-sheets.

In addition to the Aβ peptides associated with Alzheimer's disease, glycine is also present at critical positions in the sequences of other peptides that form insoluble fibrils and are associated with human diseases. Two important examples are the proteins associated with Parkinson's disease and with transmissible spongiform encephalopathies. α-Synuclein, the protein associated with Parkinson's disease, has α-helical secondary structure that converts to β-sheet structure upon fibril formation (*30*). The highly fibrillogenic core (residues 60−85) contains several glycines in the context of a long stretch of hydrophobic, mostly β-branched, amino acids. This sequence has a parallel, in-register arrangement as in GpA_{70-86} and $Aβ_{1-42}$ (*31*) and contains at least one GxxxG motif. The prion protein is a classic example of a misfolded protein that forms insoluble plaques in the brain. Cohen and Pruisner (*32*) predict that a glycine-rich sequence (residues 113−135) adopts a parallel β-helical architecture in the infectious isoform of the protein, PrPsc. This 23-residue sequence corresponds to the membrane-spanning segment in one topological form of the normal PrP protein (*33*). Like the TM region of glycophorin A, an 18 amino acid peptide (residues 118−135) of PrP is fibrillogenic (*34*), and strikingly has three consecutive GxxxG motifs. Finally, the transmembrane domain of surfactant protein SPC has a VGALLMGL sequence that is similar to that of the dimerization region of glycophorin A (*35*), but with an AxxxG motif, and is able to form fibrils when no longer associated with membrane bilayers (*36*).

The lack of sequence identity between these and other fibril-forming peptides led Chiti et al. (*37*) to suggest that amyloid fibrils are stabilized by main chain interactions, a mechanism that would be entirely consistent with the prevalence of glycine in all of these proteins. However, as indicated above, the GxxxG motif, per se, is not necessary for amyloid formation, and may simply reflect its overrepresentation in transmembrane sequences (*9*). In this regard, Dobson and colleagues have shown that a wide range of proteins can form amyloid-like fibrils under the appropriate conditions (*38*). In the case of the α/β protein acylphosphatase, they characterized the rate of conversion of 40 single-point mutants into protofibrils or granules in a sequence of events leading to full amyloid-like fibrils (*39*). The mutation that caused the greatest increase in rate was A30G (*39*), a position that is in the first α-helix of the native protein.

Together with our previous studies showing the importance of glycine in mediating helix−helix interactions in membrane proteins (*7*), the current findings reveal a remarkable structural versatility for glycine which appears to be dependent on the nature of the protein sequence and its environment. In soluble proteins, glycine has a high propensity for reverse turns, particularly within peptide sequences containing highly polar amino acids. In membrane proteins, glycine and the β-branched amino acids (Thr, Ile, Val) are overrepresented in transmembrane helices (*8*). The role of glycine in these situations is to mediate helix−helix interactions (*7*). In contrast, glycine and the β-branched amino acids have lower occurrences in helices of soluble proteins (*8*). Glycine has a relatively low occurrence in β-sheet secondary structure as well, where β-branched amino acids are favored. The combination of glycine and β-branched amino acids appears to be favorable for the formation of β-sandwich structures and amyloid-like fibrils. When hydrophobic sequences containing these amino acids are found in aqueous environments, we propose that glycine facilitates the conversion to β-strand secondary structure and can form molecular notches or grooves on the surface of β-sheets that mediate sheet-to-sheet packing. We show that these structural features can be exploited for the rational design of inhibitors to disrupt fibril formation.

ACKNOWLEDGMENT

We thank Martine Ziliox for assistance with the NMR experiments and critical reading of the manuscript, and Dan

Raleigh for insightful discussions about glycine and protein misfolding.

SUPPORTING INFORMATION AVAILABLE

Table 1 showing the amino acid preferences for β-sandwich secondary structure compared to preferences for β-strand secondary structure (PDF). This material is available free of charge via the Internet at http://pubs.acs.org.

REFERENCES

1. Glenner, G. G., and Wong, C. W. (1984) Alzheimers-disease and downs-syndrome—sharing of a unique cerebrovascular amyloid fibril protein, *Biochem. Biophys. Res. Commun. 122*, 1131−1135.
2. Glenner, G. G., and Wong, C. W. (1984) Alzheimers-disease—initial report of the purification and characterization of a novel cerebrovascular amyloid protein, *Biochem. Biophys. Res. Commun. 120*, 885−890.
3. Selkoe, D. J. (1999) Translating cell biology into therapeutic advances in Alzheimer's disease, *Nature 399*, A23-A31.
4. De Strooper, B., and Konig, G. (2001) Alzheimer's disease—An inflammatory drug prospect, *Nature 414*, 159−160.
5. Jarrett, J. T., Berger, E. P., and Lansbury, P. T. (1993) The carboxy terminus of the β-amyloid protein is critical for the seeding of amyloid formation—implications for the pathogenesis of Alzheimers-disease, *Biochemistry 32*, 4693−4697.
6. Dalal, S., Balasubramanian, S., and Regan, L. (1997) Transmuting α helices and β sheets, *Folding Des. 2*, R71−R79.
7. Javadpour, M. M., Eilers, M., Groesbeek, M., and Smith, S. O. (1999) Helix packing in polytopic membrane proteins: role of glycine in transmembrane helix association, *Biophys. J. 77*, 1609−1618.
8. Eilers, M., Patel, A. B., Liu, W., and Smith, S. O. (2002) Comparison of helix interactions in membrane and soluble α-bundle proteins, *Biophys. J. 82*, 2720−2736.
9. Senes, A., Gerstein, M., and Engelman, D. M. (2000) Statistical analysis of amino acid patterns in transmembrane helices: The GxxxG motif occurs frequently and in association with β-branched residues at neighboring positions, *J. Mol. Biol. 296*, 921−936.
10. Russ, W. P., and Engelman, D. M. (2000) The GxxxG motif: a framework for transmembrane helix-helix association, *J. Mol. Biol. 296*, 911−919.
11. Lemmon, M. A., Flanagan, J. M., Treutlein, H. R., Zhang, J., and Engelman, D. M. (1992) Sequence specificity in the dimerization of transmembrane α-helices, *Biochemistry 31*, 12719−12725.
12. MacKenzie, K. R., Prestegard, J. H., and Engelman, D. M. (1996) Leucine side-chain rotamers in a glycophorin A transmembrane peptide as revealed by three-bond carbon-carbon couplings and ^{13}C chemical shifts, *J. Biomol. NMR 7*, 256−260.
13. Smith, S. O., Song, D., Shekar, S., Groesbeek, M., Ziliox, M., and Aimoto, S. (2001) Structure of the transmembrane dimer interface of glycophorin A in membrane bilayers, *Biochemistry 40*, 6553−6558.
14. LeVine, H. (1999) Quantification of β-sheet amyloid fibril structures with thioflavin T, *Methods Enzymol. 309*, 274−284.
15. Metz, G., Wu, X., and Smith, S. O. (1994) Ramped-amplitude cross polarization in magic angle spinning NMR, *J. Magn. Reson., A 110*, 219−227.
16. Bennett, A. E., Rienstra, C. M., Auger, M., Lakshmi, K. V., and Griffin, R. G. (1995) Heteronuclear decoupling in rotating solids, *J. Chem. Phys. 103*, 6951−6958.
17. Takegoshi, K., Nakamura, S., and Terao, T. (2001) C-13-H-1 dipolar-assisted rotational resonance in magic-angle spinning NMR, *Chem. Phys. Lett. 344*, 631−637.
18. Crocker, E., Patel, A. B., Eilers, M., Jayaraman, S., Getmanova, E., Reeves, P. J., Ziliox, M., Khorana, H. G., Sheves, M., and Smith, S. O. (2004) Dipolar assisted rotational resonance NMR of tryptophan and tyrosine in rhodopsin, *J. Biomol. NMR 29*, 11−20.
19. Orengo, C. A., Michie, A. D., Jones, S., Jones, D. T., Swindells, M. B., and Thornton, J. M. (1997) CATH—a hierarchic classification of protein domain structures, *Structure 5*, 1093−1108.
20. Williams, R. W., Chang, A., Juretic, D., and Loughran, S. (1987) Secondary structure predictions and medium range interactions, *Biochim. Biophys. Acta 916*, 200−204.
21. Smith, S. O., Jonas, R., Braiman, M., and Bormann, B. J. (1994) Structure and orientation of the transmembrane domain of glycophorin A in lipid bilayers, *Biochemistry 33*, 6334−6341.
22. Sunde, M., and Blake, C. C. F. (1998) From the globular to the fibrous state: protein structure and structural conversion in amyloid formation, *Q. Rev. Biophys. 31*, 1−39.
23. Castellani, F., van Rossum, B., Diehl, A., Schubert, M., Rehbein, K., and Oschkinat, H. (2002) Structure of a protein determined by solid-state magic-angle-spinning NMR spectroscopy, *Nature 420*, 98−102.
24. Burkoth, T. S., Benzinger, T. L. S., Urban, V., Morgan, D. M., Gregory, D. M., Thiyagarajan, P., Botto, R. E., Meredith, S. C., and Lynn, D. G. (2000) Structure of the β-amyloid(10-35) fibril, *J. Am. Chem. Soc. 122*, 7883−7889.
25. Jaroniec, C. P., MacPhee, C. E., Astrof, N. S., Dobson, C. M., and Griffin, R. G. (2002) Molecular conformation of a peptide fragment of transthyretin in an amyloid fibril, *Proc. Natl. Acad. Sci. U.S.A. 99*, 16748−16753.
26. Antzutkin, O. N., Balbach, J. J., Leapman, R. D., Rizzo, N. W., Reed, J., and Tycko, R. (2000) Multiple quantum solid-state NMR indicates a parallel, not antiparallel, organization of β-sheets in Alzheimer's β- amyloid fibrils, *Proc. Natl. Acad. Sci. U.S.A. 97*, 13045−13050.
27. Takegoshi, K., Nakamura, S., and Terao, T. (2003) C-13-H-1 dipolar-driven C-13-C-13 recoupling without C-13 rf irradiation in nuclear magnetic resonance of rotating solids, *J. Chem. Phys. 118*, 2325−2341.
28. Smith, S. O., and Bormann, B. J. (1995) Determination of helix-helix interactions in membranes by rotational resonance NMR, *Proc. Natl. Acad. Sci. U.S.A. 92*, 488−491.
29. Wang, L., Oconnell, T., Tropsha, A., and Hermans, J. (1996) Molecular simulations of β-sheet twisting, *J. Mol. Biol. 262*, 283−293.
30. Kessler, J. C., Rochet, J. C., and Lansbury, P. T. (2003) The N-terminal repeat domain of α-synuclein inhibits β-sheet and amyloid fibril formation, *Biochemistry 42*, 672−678.
31. Der-Sarkissian, A., Jao, C. C., Chen, J., and Langen, R. (2003) Structural organization of alpha-synuclein fibrils studied by site-directed spin labeling, *J. Biol. Chem. 278*, 37530−37535.
32. Govaerts, C., Wille, H., Prusiner, S. B., and Cohen, F. E. (2004) Evidence for assembly of prions with left-handed beta 3-helices into trimers, *Proc. Natl. Acad. Sci. U.S.A. 101*, 8342−8347.
33. Hegde, R. S., Mastrianni, J. A., Scott, M. R., DeFea, K. A., Tremblay, P., Torchia, M., DeArmond, S. J., Prusiner, S. B., and Lingappa, V. R. (1998) A transmembrane form of the prion protein in neurodegenerative disease, *Science 279*, 827−834.
34. Florio, T., Paludi, D., Villa, V., Principe, D. R., Corsaro, A., Millo, E., Damonte, G., D′Arrigo, C., Russo, C., Schettini, G., and Aceto, A. (2003) Contribution of two conserved glycine residues to fibrillogenesis of the 106-126 prion protein fragment. Evidence that a soluble variant of the 106-126 peptide is neurotoxic, *J. Neurochem. 85*, 62−72.
35. Kairys, V., Gilson, M. K., and Luy, B. (2004) Structural model for an AxxxG-mediated dimer of surfactant-associated protein C, *Eur. J. Biochem. 271*, 2086−2092.
36. Gustafsson, M., Thyberg, J., Naslund, J., Eliasson, E., and Johansson, J. (1999) Amyloid fibril formation by pulmonary surfactant protein C, *FEBS Lett. 464*, 138−142.
37. Chiti, F., Webster, P., Taddei, N., Clark, A., Stefani, M., Ramponi, G., and Dobson, C. M. (1999) Designing conditions for in vitro formation of amyloid protofilaments and fibrils, *Proc. Natl. Acad. Sci. U.S.A. 96*, 3590−3594.
38. Fandrich, M., Fletcher, M. A., and Dobson, C. M. (2001) Amyloid fibrils from muscle myoglobin—Even an ordinary globular protein can assume a rogue guise if conditions are right, *Nature 410*, 165−166.
39. Chiti, F., Taddei, N., Baroni, F., Capanni, C., Stefani, M., Ramponi, G., and Dobson, C. M. (2002) Kinetic partitioning of protein folding and aggregation, *Nat. Struct. Biol. 9*, 137−143.

BI047827G